The Astrophysical Journal, 766:83 (15pp), 2013 April 1 doi:10.1088/0004-637X/766/2/83

GAMMA-RAY OBSERVATIONS OF CYGNUS X-1 ABOVE 100 MeV IN THE HARD AND SOFT STATES

S. Sabatini[1,2], M. Tavani[1,2,3], P. Coppi[4], G. Pooley[5], M. Del Santo[1], R. Campana[1,6], A. Chen[7], Y. Evangelista[1], G. Piano[1,2], A. Bulgarelli[6], P. W. Cattaneo[8], S. Colafrancesco[9], E. Del Monte[1], A. Giuliani[7], M. Giusti[1], F. Longo[10], A. Morselli[2,3], A. Pellizzoni[11], M. Pilia[12], E. Striani[1,3], M. Trifoglio[6], and S. Vercellone[13]
[1] INAF/IAPS-Roma, I-00133 Roma, Italy
[2] INFN Roma Tor Vergata, I-00133 Roma, Italy
[3] Dip. di Fisica, Univ. Tor Vergata, I-00133 Roma, Italy
[4] Yale University, P.O. Box 208101, New Haven, CT 06520-8101, USA
[5] Cavendish Laboratory, University of Cambridge, Cambridge CB3 0HE, UK
[6] INAF/IASF-Bologna, I-40129 Bologna, Italy
[7] INAF/IASF-Milano, I-20133 Milano, Italy
[8] INFN-Pavia, I-27100 Pavia, Italy
[9] INAF-OAR, I-00040 Monteporzio Catone, Italy
[10] Dip. Fisica and INFN Trieste, I-34127 Trieste, Italy
[11] INAF-OAC, I-09012 Capoterra, Italy
[12] ASTRON, The Netherlands Institute for Radio Astronomy, Postbus 2, 7990 AA, Dwingeloo, The Netherlands
[13] INAF/IASF-Palermo, I-90146 Palermo, Italy
Received 2012 October 3; accepted 2013 February 8; published 2013 March 12

ABSTRACT

We present the results of multi-year gamma-ray observations by the *AGILE* satellite of the black hole binary system Cygnus X-1. In a previous investigation we focused on gamma-ray observations of Cygnus X-1 in the hard state during the period mid-2007/2009. Here we present the results of the gamma-ray monitoring of Cygnus X-1 during the period 2010/mid-2012 which includes a remarkably prolonged "soft state" phase (2010 June–2011 May). Previous 1–10 MeV observations of Cyg X-1 in this state hinted at a possible existence of a non-thermal particle component with substantial modifications of the Comptonized emission from the inner accretion disk. Our *AGILE* data, averaged over the mid-2010/mid-2011 soft state of Cygnus X-1, provide a significant upper limit for gamma-ray emission above 100 MeV of $F_{\rm soft} < 20 \times 10^{-8}$ photons cm^{-2} s^{-1} , excluding the existence of prominent non-thermal emission above 100 MeV during the soft state of Cygnus X-1. We discuss theoretical implications of our findings in the context of high-energy emission models of black hole accretion. We also discuss possible gamma-ray flares detected by *AGILE*. In addition to a previously reported episode observed by *AGILE* in 2009 October during the hard state, we report a weak but important candidate for enhanced emission which occurred at the end of 2010 June (2010 June 30 10:00–2010 July 2 10:00 UT) exactly coinciding with a hard-to-soft state transition and before an anomalous radio flare. An appendix summarizes all previous high-energy observations and possible detections of Cygnus X-1 above 1 MeV.

Key words: black hole physics – gamma rays: general – stars: flare – stars: individual (Cygnus X-1) – stars: winds, outflows – X-rays: binaries

Online-only material: color figures

1. INTRODUCTION

Cygnus X-1 (Cyg X-1) is the archetypal black hole binary system in our Galaxy. It is composed of a compact object and a O9.7 Iab supergiant star companion with a mass estimate ranging between ∼17–31 $M_{\odot}$, filling 97% of its Roche lobe (Gierlinski et al. 1999; Caballero-Nieves et al. 2009). The measurements of the mass for the compact object range from 4.8 to 14.8 $M_{\odot}$ (Herrero et al. 1995; Shaposhnikov & Titarchuk 2007; Orosz et al. 2011), suggesting identification with a black hole. Being one of the brightest sources in the X-ray sky and having a persistent emission, the literature on the system is extremely rich and extensive monitoring in radio, IR, UV, and X-rays has been carried out (Mirabel et al. 1996; Pooley et al. 1999; Fender et al. 2000; McConnell et al. 2002; Gallo et al. 2003; Pandey et al. 2006; Del Monte et al. 2010; Rahoui et al. 2011; Jourdain et al. 2012), leading to interesting correlations and being of great importance for understanding the process of accretion onto black holes in general.

Typical X-ray spectral states of Cyg X-1 have been classified into the "hard/low" and "soft/high" states, which are defined according to the spectral behavior at X-ray energies (<20 keV). The source usually spends 90% of its time in the low/hard spectral state whose spectral energy distribution is well described by a power law ($E^{-\gamma}$) with photon index $\gamma \sim 1.7$, a very prominent broad emission peak of the power spectral energy density (νF_{ν}) near 100 keV, and a high-energy cutoff at ∼150 keV. The less common soft state is characterized by the absence of the prominent peak near 100 keV, a strong blackbody component with $kT \sim 0.5$ keV, and a soft power-law tail with γ usually ranging between 2 and 3. Intermediate spectral states also exist (see, e.g., Belloni et al. 1996) and a number of different spectral shapes have been reported in the literature (e.g., *INTEGRAL* observations; Del Santo et al. 2013 and references therein).

The different spectral states are usually described by the interplay of a relatively cool accretion disk and a hot optically thick corona surrounding the central source. In the hard state, the spectral energy distribution can be modeled by Comptonization of abundant soft blackbody photons from the inner accretion disk which scatter off the energetic electrons of the optically thick corona (e.g., Coppi 1999, 2004; Zdziarski et al. 2002, 2011, 2012; Zdziarski & Gierlinski 2004). A crucial

property of this corona, energized by the accretion process onto the black hole, is its ability to add a non-thermal tail to an otherwise thermal distribution of electrons, possibly extending to the gamma-ray energy range. This process of non-thermal energization of coronal electrons is strongly constrained in the Cyg X-1 hard states by the apparent cutoff observed above 150 keV (Gierlinski et al. 1997; McConnell et al. 2002) and by the absence of detectable gamma-ray emission above 100 MeV (Sabatini et al. 2010b). In the transition to the soft state, the Comptonizing corona shrinks, the cool disk moves inward (possibly very close to the last stable orbit), and non-thermal processes, if existing, can be revealed by emission above the disk blackbody component, in particular with the detection of prominent power-law components above the MeV energy range in the soft spectral state.

For many years, the only available information on the spectral states of Cyg X-1 above MeV energies was the data collected by the COMPTEL instrument on board the *Compton Gamma-Ray Observatory* (*CGRO*; Collmar, 2003). Cyg X-1 remained in the hard state for most of the *CGRO* observations, as monitored by the hard X-ray instrument BATSE (McConnell et al. 2002). However, during the *CGRO* lifetime, two transitions to Cyg X-1 soft states were studied by the combined effort of the OSSE, COMPTEL, and EGRET instruments (see the Appendix for more details of these important observations). Cyg X-1 transitions to the soft state are relatively rare (e.g., Zhang et al. 1997a) and not well understood theoretically. A very significant non-thermal emission episode was detected by COMPTEL in one case[14] with a maximum photon energy recorded at 5–10 MeV (McConnell et al. 1997, 2002). This detection was for many years the only indication of a possible non-thermal component in the soft state spectrum of Cyg X-1, and stimulated many investigations and speculations about its nature (Gierlinski et al. 1999; Zdziarski et al. 2002). In particular, the detection of emission up to 100 MeV and beyond would test hybrid Comptonization spectral models of black hole emission. As a result, there has been great interest in new gamma-ray data from Cyg X-1 in a soft state by the current generation of gamma-ray space instruments (*AGILE* and *Fermi*).

In a previous paper we reported on the gamma-ray observations of Cyg X-1 by the *AGILE* satellite that were obtained during the period 2007–2009, during which the source was in a prolonged hard state (Sabatini et al. 2010b). Here we present the results of the *AGILE* gamma-ray monitoring of Cyg X-1 during the 2010/mid-2012 period. This period includes the 2010 June event during which the system underwent a clear spectral transition from the hard to the soft state and unusually remained in the soft state for almost a year. This gave us the unprecedented opportunity to carry out a long-term monitoring of the soft spectral state of Cyg X-1 at gamma-ray energies and investigate the possible existence of prominent emission above 100 MeV.

Gamma-ray data in the Cyg X-1 soft state are of crucial importance for theoretical modeling because they constrain the high-energy part of the spectrum, which is most likely dominated by non-thermal emission. Of particular interest are observations that can determine a clear cutoff in the spectra at high energies, since the cutoff energy is a function of the compactness of the inner source region.

For a proper evaluation of the physical properties of Cyg X-1 in different accretion states, it is important to consider also radio and X-ray emission in addition to gamma-ray data above 50 MeV. In particular, for many years Cyg X-1 has been monitored in search of non-thermal radio jets. Radio emission is observed to be persistent with a modulation related to the orbital period of the system (Zhang et al. 1997b; Stirling et al. 2001) during the hard states and presents a strong decrease during soft states (see, e.g., Zdziarski et al. 2011). Definitive evidence for a resolved extended relativistic radio jet was provided by Stirling et al. (2001) using Very Long Baseline Array and MERLIN data. Fender (2001) estimated an angle of 30° between the jet axis and the line of sight, assuming the jet to be perpendicular to the disk. A more recent estimate for the angle of inclination of the orbital plane to our line of sight is $27.^{\circ}1 \pm 0.^{\circ}8$ (Orosz et al. 2011). A jet bulk Lorentz factor of $\Gamma = (1-\beta^2)^{-1/2} \simeq 1.25$ and a jet kinetic power $P_{\rm j} \simeq (1\text{–}3) \times 10^{37}\,{\rm erg\,s^{-1}}$ have been determined in the hard state from the large-scale optical emission of a nebula most likely energized by the Cyg X-1 jet (Gallo et al. 2005; Russell et al. 2007; see also Gleissner et al. 2004; Malzac et al. 2009; and the discussion in Zdziarski et al. 2012).

Cyg X-1 has been repeatedly observed in X-rays both in the hard and soft states. Of particular interest are the *INTEGRAL* observations of Cyg X-1 that cover the energy range 20 keV–1 MeV (see the recent review and discussion by Zdziarski et al. 2012 who also reconsider the spectral data of Laurent et al. 2011). An important aspect of high-energy emission from Cyg X-1 is its variability. Variability in the X-ray band has been observed on several different timescales (Brocksopp et al. 1999; Pottschmidt et al. 2003; Ling et al. 1997; Golenetskii et al. 2003). Several outburst episodes in both the hard and soft states at various orbital phases were also reported by Golenetskii et al. (2003) using the Interplanetary Network in the 15–300 keV band and by Gierlinski & Zdziarski (2003) in the *RXTE*/PCA 3–30 keV data. Variability of the high-energy emission from Cyg X-1 is indeed a crucial issue. More recently very fast transient activity (on the order of hours) was also detected at the TeV energy range by the MAGIC telescope (Albert et al. 2007), and in the radio frequency by the MERLIN and Ryle telescopes (Fender et al. 2006).

For a black hole mass $M \sim 10\,M_{\odot}$, both the total X-ray emission $L_{\rm X} \simeq 10^{37}\,{\rm erg\,s^{-1}}$ and jet kinetic power in the hard state P_j indicate sub-Eddington accretion conditions. Data in the soft state of Cyg X-1 show that the X-ray luminosity can be similar or typically higher and a low-level jet activity can be present during this radio quenched state (Rushton et al. 2011, 2012; see also below and the Appendix A.1). In general, we can distinguish two types of gamma-ray emission from a black hole system such as Cyg X-1: (1) "accretion-driven emission," with X-rays and possibly gamma-rays originating from the inner accretion disk and/or Comptonizing corona (2) and "jet emission" originating in the accelerating flow of the jet.[15] The interpretation of the 1–10 MeV emission and above plays a crucial role. This spectral component, detected both in the hard and in the soft states of Cyg X-1 (see below), can be attributed either to hybrid Comptonization of accretion-driven emission or to a synchrotron tail of jet emission (e.g., Zdziarski et al. 2012). In this paper we focus specifically on the gamma-ray emission of the Cyg X-1 soft state during which jet activity is

[14] In the following, we are going to take the COMPTEL detection of Cyg X-1 in the soft state reported by McConnell et al. (2002) as a typical soft-state emission by a non-thermal component.

[15] Interaction of a non-thermal relativistic jet with the ambient photon fields from the accretion disk, the corona, and the companion star wind contributing to the high-energy band of the spectrum (hard X-rays γ-rays) can be modeled both in hadronic (Romero et al. 2003; Perucho & Bosch-Ramon 2008) or leptonic scenarios (Perucho & Bosch-Ramon 2008; Piano et al. 2012; Zdziarski et al. 2012; Zdziarski 2012).

in general subdued compared to the hard state (see, e.g., Fender et al. 2004). We therefore aim here at constraining the possible existence of an accelerated population of electrons/positrons for the accretion-driven scenario.

Section 2 reviews the *AGILE* gamma-ray observations of Cyg X-1 in the hard state as well as during the recent prolonged (almost 1 year long) soft state period. We present in Section 3 the theoretical implications of our upper limits to the emission above 100 MeV. Section 4 presents a general discussion of the accretion-driven high-energy emission from Cyg X-1. We find it useful to summarize all relevant previous gamma-ray observations and detections of Cyg X-1 above 1 MeV in the Appendix. We also present there two transient episodes of gamma-ray emission from Cyg X-1 that at the moment constitute noticeable exceptions to the standard low-intensity gamma-ray state. In particular, we present data on a new relatively low-intensity/low-significance episode of emission that occurred just prior to a major X-ray and radio flaring transition on 2010 June 30 to July 2.

2. *AGILE* OBSERVATIONS AND RESULTS

The *AGILE* gamma-ray astrophysics mission has been operating since 2007 April (Tavani et al. 2008). The *AGILE* scientific instrument is very compact and is characterized by two co-aligned imaging detectors operating in the energy ranges 30 MeV–30 GeV (the imaging gamma-ray detector—*GRID*; Barbiellini et al. 2002; Prest et al. 2003; Bulgarelli et al. 2010) and 18–60 keV (the hard X-ray detector *Super-AGILE*; Feroci et al. 2007). An anticoincidence system (Perotti et al. 2006) and a calorimeter sensitive in the 0.4–100 MeV energy range (Labanti et al. 2006) complete the instrument. *AGILE*'s performance is characterized by large fields of view (2.5 and 1 sr for the gamma-ray and hard X-ray bands, respectively), good sensitivity in pointing mode[16] near 100 MeV (the on-axis effective area is about 400 cm^2 at 100 MeV), and state-of-the-art angular resolution (68% containment radius point spread function (PSF) $\sim 3.^\circ5$ at 100 MeV and PSF $\sim 1.^\circ5$ at 400 MeV).

Flux sensitivity for a typical one-week observation in pointing mode can reach the level of $F \sim (20\text{–}30) \times 10^{-8}$ photons cm^{-2} s^{-1} above 100 MeV depending on off-axis angles and pointing directions (see Tavani et al. 2008 for details about the mission and main instrument performance).

AGILE observed the Cygnus region in the Galactic plane several times during the period 2007 July–2011 May (Sabatini et al. 2010b; Chen et al. 2011; Piano et al. 2012). Figure 1 shows the daily monitoring in the soft (ASM 1.3–12.2 keV) and hard (*Swift*-BAT 15–50 keV) X-ray range. *AGILE* observation intervals of the Cygnus region in pointing (dark gray) and spinning (light gray) modes are shown. The transition to (and persistence in) the soft state starting around MJD 55380 is evident. In a previous paper (Sabatini et al. 2010b) we analyzed our pointing mode data up to the end of 2009 (MJD 55120). Here we focus on the 2010 June–2011 May period, during which Cyg X-1 was entirely in the soft state.

The analysis of the gamma-ray data presented in this paper was carried out with the standard *AGILE-GRID* FM3.119 filter_I0010 B20 calibrated filter with a gamma-ray event selection that takes into account South Atlantic Anomaly event cuts and 80° Earth albedo filtering. Throughout the paper, statistical significance and source flux were determined using the standard *AGILE* multi-source likelihood analysis software (Bulgarelli et al. 2012a). The statistical significance is expressed in terms of a Test Statistic (Mattox et al. 1996) and asymptotically distributed as a $\chi^2/2$ for 3 degrees of freedom ($\chi^2_3/2$). We assessed the pre- and post-trial significance using multiple Monte Carlo simulations of the sensitivity of the gamma-ray instrument to point-like source emission (Bulgarelli et al. 2012a).

Figure 2 shows the *AGILE* deep gamma-ray integrations of the Cygnus region above 100 MeV during the periods 2007 July–2010 October (MJD: 54406–55121) and 2010 June–2011 May (MJD: 55378–55647), covering the hard and the soft spectral state, respectively. No gamma-ray persistent emission from Cyg X-1 was detected by *AGILE* during either spectral states of the source for these deep integrations. A multi-source likelihood analysis, including all known gamma-ray sources of the region, provides a 2σ upper limit for the energy $\geqslant$100 MeV of $F_{\rm UL,hard} = 3 \times 10^{-8}$ photons cm^{-2} s^{-1} for the hard state (Sabatini et al. 2010b) and $F_{\rm UL,soft} = 20 \times 10^{-8}$ photons cm^{-2} s^{-1} for the soft state. Figure 3 shows typical hard and soft spectral states from the literature (e.g., McConnell et al. 2002) together with the *AGILE* upper limits (plotted in red). For the soft state, we also plot in Figure 3 (bottom panel) the soft gamma-ray emission detected on one occasion by COMPTEL (McConnell et al. 2002; see also the discussion in the Appendix).

The *AGILE* gamma-ray upper limit in the soft state is quite important, and excludes a simple power-law extrapolation of the soft gamma-ray emission detected by COMPTEL. Both measurements, obtained with *AGILE* data after many months of observations, confirm that Cyg X-1 is not a steady gamma-ray emitter above 100 MeV at levels comparable to those detected from the other prominent micro-quasar Cygnus X-3 (Tavani et al. 2009; Abdo et al. 2009; Bulgarelli et al. 2012b; Corbel et al. 2012; Piano et al. 2012). These findings have important theoretical implications, which we discuss in the next section.

3. *RXTE* PCA/HEXTE DATA

Nineteen pointed observations were performed by *RXTE* PCA/HEXTE during the period 2010 June 19–July 31, for a net exposure time of about 68.5 ks, catching the source across the whole transition from the hard to the soft state. The change of state can be described by a change in the Power Density Spectra (PDS) as shown in Figure 9 in the Appendix and here we adopt Shaposhnikov & Titarchuk (2006) nomenclature for the classification of spectral states. The fractional rms dropped to about 4% on 2010 July 4, which clearly shows that the source had finally reached the soft state. Figure 4 shows *RXTE* PCA/HEXTE data of the July 4 and 22, when the source was respectively in the soft and super-soft state, during the *AGILE* monitoring.

4. RESULTS AND DISCUSSION

The lack of detectable gamma-ray flux above 100 MeV from Cyg X-1 in the soft state leads to important theoretical constraints. Cyg X-1 has been considered to be a crucial test case for the modeling of radiation mechanisms of accreting black holes in the literature (Coppi 1999; Gierlinski et al. 1999; Zdziarski et al. 2012 and references therein). From the properties of the soft X-ray and hard X-ray emission and the well-defined pattern of spectral state changes, Comptonization models have been successfully applied to describe the high-energy emission

[16] *AGILE* operated in pointing mode during the first phase of operations (2007 July–mid 2009 October). Since 2010 January the satellite has been operating in "spinning" mode, observing a large fraction of the sky continuously with somewhat reduced sensitivity per unit time but much increased overall sky coverage.

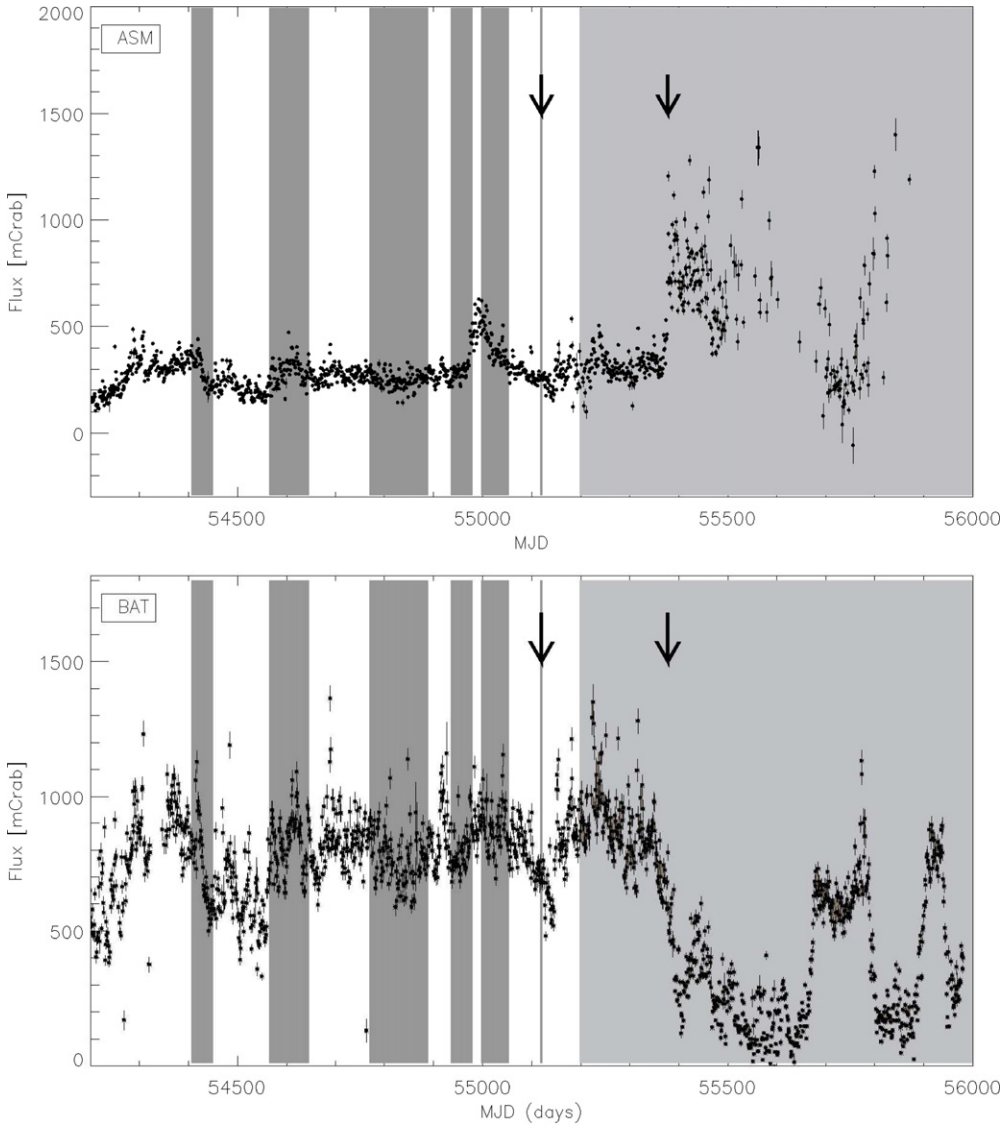

Figure 1. Long-term daily monitoring of Cyg X-1 in the soft and hard X-ray bands. Upper panel shows *RXTE*-ASM data in the 1.3–12.2 keV energy range; lower panel shows *Swift*-BAT data in the 15–50 keV energy range. The gray areas show *AGILE* observing intervals covering the Cygnus region: dark gray regions refer to the pointing mode and light gray to the spinning mode of the satellite, respectively. Black arrows show the gamma-ray flares observed by *AGILE* as reported in this paper.

from Cyg X-1 (e.g., Coppi 1999; Poutanen & Coppi 1998; Zdziarski et al. 2002, 2012). In this approach, different spectral states of the source are interpreted in relation to the interplay between the emission from an optically thick, cold accretion disk, and a geometrically thin/optically thick corona above the disk. In the simplest versions of this model, the high-energy emission of the soft state is expected to be steady and possibly to extend up to gamma-ray energies above 1 MeV depending on the details of the thermal versus non-thermal electron/positron component in the Comptonized corona. The disk contributes typically to the soft photon emission with a thermal distribution of temperature T_s and luminosity L_s. The corona is a much more complex and dynamical system where non-thermal particle acceleration, electron/positron pair formation and annihilation, optically thick Comptonization of thickness τ, and inverse Compton scattering occur. It is customary to define a "hard luminosity" L_h that takes into account the emission originating from these processes. Comptonization modeling using the EQPAIR numerical code (Coppi 1999) treats these processes self-consistently, and can be used for the interpretation of Cyg X-1 observations. The system "compactness parameter" l defined as $l = L\sigma_T/Rm_ec^3$ plays a crucial role, where L is the luminosity of interest ("soft" or "hard"), σ_T is the Thomson cross section, R is the typical radius of interest (either the inner disk and/or the corona), m_e is the electron's mass, and c is the speed of light. Depending on the choice of L_s or L_h (and in principle of the corresponding emitting radius R) we can define the "soft" (l_s) and "hard" (l_h) compactness parameters. Constraining these values for the typical emission of Cyg X-1 has been a long-standing theoretical problem.

The soft component of the spectrum is modeled by blackbody disk emission with l_s related to the power supplied in the form of soft seed photons, while the hard tail is attributed to the corona, where photons from the disk repeatedly Compton scatter off electrons with a hybrid thermal/non-thermal distribution. Electron contributions are then parameterized by the compactness parameters for thermal ($l_{\rm th}$) and non-thermal ($l_{\rm nth}$) electrons, and we can define a compactness parameter for the total power supplied to the electrons, $l_h = l_{\rm th} + l_{\rm nth}$. Typically, the corona non-thermal compactness has comparable value in

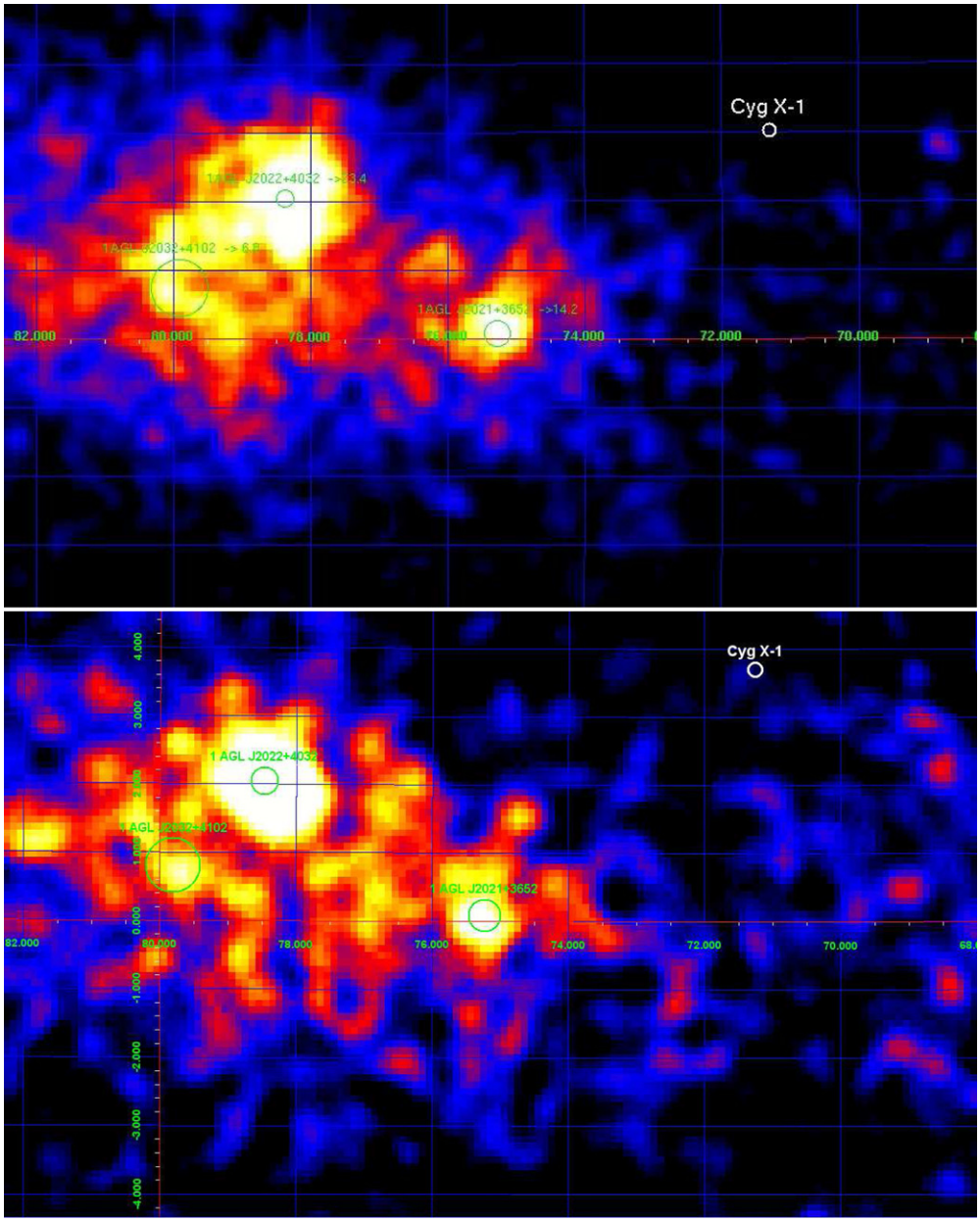

Figure 2. *AGILE* gamma-ray deep intensity maps above 100 MeV of the Cygnus region in Galactic coordinates displayed with a three-bin Gaussian smoothing. Pixel size is 0.°1 and the nominal position of Cyg X-1 is marked in white. Upper panel: an integration of *AGILE* data covering all the data of the pointing mode (2007–2009), when Cyg X-1 was in the hard state. Lower panel: deep integration of *AGILE* data in spinning mode selecting the time intervals during which Cyg X-1 was in the soft state (MJD 55378–55647, see Figure 1).

(A color version of this figure is available in the online journal.)

both hard and soft Cyg X-1 spectral states ($l_{\rm nth} \sim 5$; Malzac & Renaud 2010); on the contrary, most of the difference between the two spectral states is expected to be due to a change in the soft photon compactness, l_s (Malzac & Renaud 2010).

For our analysis of the soft state, we considered a class of hybrid Comptonization models, and fitted the available data with EQPAIR, exploring how the relevant physical parameters (most importantly, the soft compactness l_s and the non-thermal to thermal compactness ratio l_h/l_s) affect the spectral energy distribution. Our first goal is to determine a model with "extreme" parameters that lead to a high-energy emission *just* consistent with our upper limit above 100 MeV. In all fits a power-law distribution of accelerated/IC-cooled electron/positron pairs is assumed ($n_{\rm inj}(\gamma) \propto \gamma^{-(\Gamma_{\rm inj}+1)}$) with an injection index $\Gamma_{\rm inj} \sim 2.7$ and minimum and maximum electron/positron Lorentz factors $\gamma_{\rm min}$ and $\gamma_{\rm max}$ fixed to the values of 1.3 and 10^3, respectively, according to the well-established literature (Gierlinski et al. 1999; Frontera et al. 2001; Del Santo et al. 2013 and references therein). The non-thermal to total hard compactness ratio $l_{\rm nth}/l_h$ is set to order of unity in order to maximize the non-thermal component. We have explored varying values of l_s in the range 1–10, letting kT_s, l_h/l_s, τ_i, and Ω be free parameters. This analysis in general produces spectra incompatible with the whole set of data for $l_s < 10$, predicting a persistent high-energy component incompatible with *AGILE* upper limit. Our constraints to the parameter space lead to a lower limit for the soft

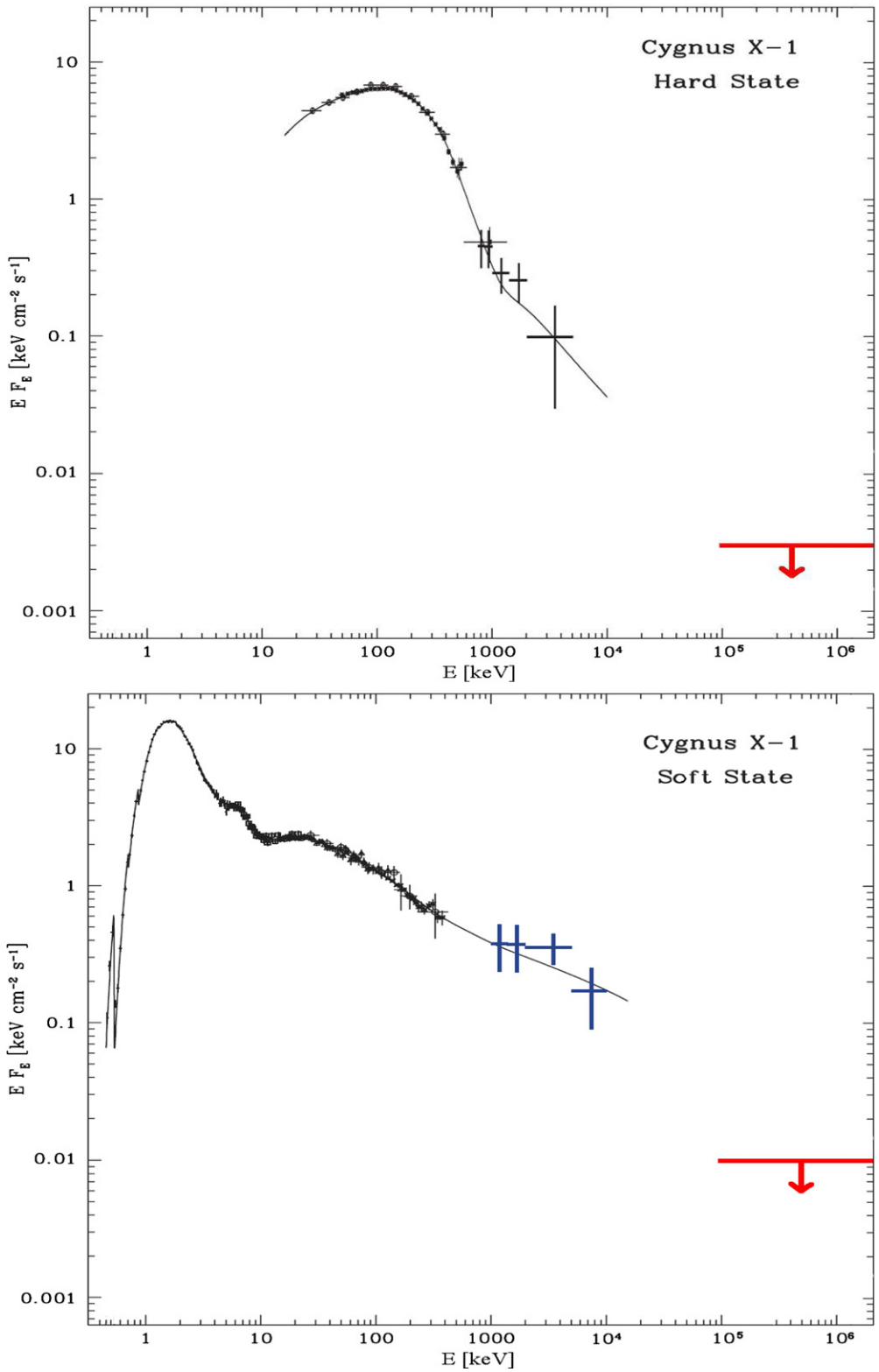

Figure 3. Spectral energy distributions of Cyg X-1 for the hard and soft states with superimposed *AGILE* upper limits (in red color). Solid lines are from McConnell et al. (2002). Upper panel: data for the hard state include OSSE and COMPTEL (COMPTEL data for this case are the average of nine different *CGRO* observations). Lower panel: data for the soft state, including LECS, HPGSPC, and PDS instruments on board *BeppoSAX* and OSSE, BATSE, and COMPTEL instruments on *CGRO* (data are for the soft state event detected in 1996 June).

(A color version of this figure is available in the online journal.)

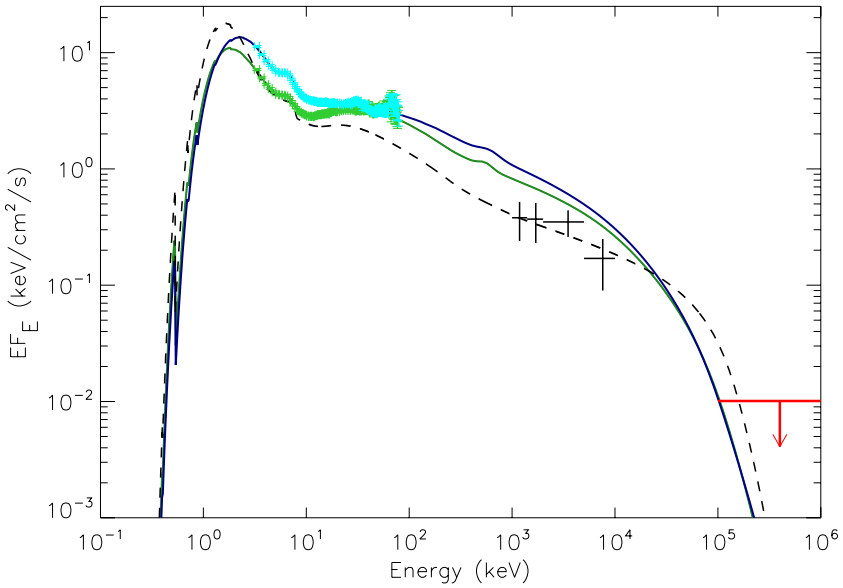

Figure 4. *AGILE* gamma-ray upper limit in the context of Cyg X-1 soft state data and modeling. *RXTE* PCA/HEXTE data during the *AGILE* monitoring are for 2010 July 4 and 22 in green and cyan, respectively. The solid line spectra are obtained with EQPAIR with the parameters of model-1 and -2, as discussed in the text. X-ray absorption is taken into account in this calculation. For comparison we also show the canonical soft state spectrum (McConnell et al. 2002) with a dashed line and COMPTEL data in black.

(A color version of this figure is available in the online journal.)

Table 1
Comptonization Model Parameters (EQPAIR) for the Soft Spectral States Shown in Figures 4 and 9

	kT_s (keV)	l_s	l_h/l_s	$l_{\rm nth}/l_h$	$\Gamma_{\rm inj}$	τ_i	$\Omega/2\pi$
model-1	$0.43^{+0.01}_{-0.04}$	(10)	$0.56^{+0.04}_{-0.07}$	(0.99)	(2.7)	0.85 ± 0.20	0.6 ± 0.1
model-2	0.65 ± 0.09	(10)	$0.57^{+0.03}_{-0.05}$	(0.99)	(2.7)	<0.3	0.3 ± 0.1
model-3	0.37	3.2	0.17	0.68	2.6	0.11	1.3

Notes. Parameters inside parentheses are frozen in the fit; free parameter errors are given at the 90% confidence level. kT_s: disk blackbody temperature; l_s: soft photon compactness; l_h/l_s: ratio of hard-to-soft compactness; $l_{\rm nth}/l_h$: ratio of non-thermal-to-total hard compactness; $\Gamma_{\rm inj}$: injection index of electron power-law distribution; τ_i: optical depth; $\Omega/2\pi$: Compton reflection. Model-1 refers to a fit to the *RXTE* PCA/HEXTE data of the soft state of 2010 July 4 (green solid line in Figure 4); model-2 is for the super-soft state of 2010 July 22 (blue solid line in Figure 4); model-3 reports McConnell et al. (2002) parameters as a reference (black dashed line in Figure 4).

compactness, which is constrained to be in the range $l_s \gtrsim 10$ in order to be simultaneously consistent with both *RXTE* data and *AGILE* upper limit, given the adopted value for $\gamma_{\rm max}$.[17] We therefore proceeded by freezing the soft inner disk component to $l_s = 10$ in order to determine the parameters reported in Table 1. We show in Figure 4 the spectral energy distributions and in Table 1 the results of the fitting procedure for the two data sets. *AGILE* upper limit obtained during the soft state is in red. Superimposed to the models are the *RXTE* PCA/HEXTE data after the spectral transition (green-colored data are for the model-1 soft state of July 4, and cyan-colored data are for the model-2 super-soft state of 2010 July 22). We also show, for comparison, in black, the historical COMPTEL gamma-ray data points for the Cyg X-1 soft state detection[18] during 1996 June, and the model by McConnell et al. (2002) for these data with a black dashed line.

We note that both "extreme" models tend to predict higher gamma-ray fluxes in the range 1–30 MeV than that measured in the historical COMPTEL detection. We note however that a more realistic modeling would require more broadband data to better constrain the values for l_s, $l_{\rm nth}/l_h$, and $\Gamma_{\rm inj}$.

Our model-1 is in qualitative agreement with model parameters explored in Gierlinski et al. (1999) for the soft state. We add the crucial information of the non-existence of a strong non-thermal component of accelerated electrons/positrons with a power-law index harder than $\Gamma_{\rm inj} = 2.7$. The ratio of l_h/l_s is well constrained to values <1, as for typical soft states. From the constraints to the soft compactness we can therefore extrapolate a range of possible values for the hard compactness (and consequently the non-thermal and thermal compactness), obtaining $l_h \gtrsim 6$.

5. CONCLUSIONS

The prolonged soft state of Cyg X-1 in mid-2010/mid-2011 offered an unprecedented opportunity to verify the existence of a prominent non-thermal tail in the gamma-ray spectrum of a black hole system accreting above 10 MeV (i.e., COMPTEL data). Our *AGILE* observations exclude the existence of such a tail. This result, combined with previous observations of Cyg X-1, confirms the physical picture of this state based on soft thermal X-ray emission emanating from the inner disk and partial reprocessing and scattering by a corona. It is interesting to note that whereas the ratio parameters l_h/l_s and $l_{\rm nth}/l_h$ are similar to previous Cyg X-1 soft states detected 1994 and 1996 (e.g., Gierlinski et al. 1999), we find a quite well-constrained value for the compactness, related to feeding soft seed photon luminosity $l_s \gtrapprox 10$. We believe that our

[17] Note that for a value of the injection index of ~2.7, higher values of $\gamma_{\rm max}$ would have negligible effects on the results, since only a small amount of power is injected at this energy. The maximum allowed value of $\gamma_{\rm max} = 10^4$ is however not completely consistent with the *AGILE* upper limit, producing some power around 100 MeV.

[18] Note that this detection constitutes a single (and so far unique) episode of emission above 1 MeV, and that another observation by COMPTEL in the soft state during 1994 January did not detect any emission from Cyg X-1.

measurements, exploring and combining data in energy ranges much broader than in past analyses, constitute the most accurate constraints on the underlying physical processes thus far.

By considering both hard and soft state upper limits to the emission from Cyg X-1, we can put our measurements in perspective. Cyg X-1 spends most of its time in a sub-Eddington optically thick hard state. Occasionally, the accreting system dramatically changes its configuration to the soft state. The overall (mostly soft X-ray) luminosity increases by a factor of up to three in magnitude (Zdziarski et al. 2002), getting closer to the Eddington luminosity. In this state, the coronal processes can be revealed more easily because of the optical thinness of the corona. We find that there are no major variations, on average, of the conditions that lead to the energization of a non-thermal population of electrons/positrons compared to the hard state. The average emission properties of Cyg X-1 at energies above 1–10 MeV appear to be quite stable.

We note that this behavior of Cyg X-1 is in contrast with even the average properties of the other prominent Galactic micro-quasar Cygnus X-3 (Tavani et al. 2009; Abdo et al. 2009). In the case of Cygnus X-3, gamma-ray emission above 100 MeV is clearly transient and originates in states with a relatively low hard X-ray flux. With the exception of two episodes of transient gamma-ray emission detected by *AGILE* from Cyg X-1 and reported in the Appendix, such an activity of recurrent and very active transient emission is not the norm in Cyg X-1.

Transient gamma-ray emission from Cyg X-1 originating from physical processes different from those of a "steady" disk+corona can be difficult to detect. The very short (less than 2 hr) TeV emission detected by MAGIC from Cyg X-1, if confirmed, is quite remarkable. The current gamma-ray missions *AGILE* and *Fermi* can detect gamma-ray variability at the level of hours only for very intense events. In the Appendix, we report one of these candidate transient events from Cyg X-1, which was detected by *AGILE* during the transition from hard-to-soft state on 2010 June 30 to July 2. If confirmed, this class of transient gamma-ray emission would open a new window into the physical processes around accreting black holes, allowing the possibility of jet or "pre-jet" launching activity of these transient events. Cyg X-1 transient gamma-ray activity could occur on short timescales (of order of the day or shorter) and with a typical gamma-ray flux of $F_\gamma \sim 100$–150×10^{-8} photons cm^{-2} s^{-1}. Such events would be difficult to detect the current generation of gamma-ray telescopes (*AGILE, Fermi*). Future instruments with an improved exposure will allow us to investigate these with events in much more detail.

We thank the anonymous referee for his/her careful reading and for the important suggestions that considerably improved the quality of the manuscript. Research partially supported by the ASI grant Nos. I/042/10/0 and I/028/12/0. M.D.S. acknowledges financial support from the agreement ASI-INAF I/009/10/0 and from PRIN-INAF 2009 (PI: L. Sidoli).

APPENDIX

A REVIEW OF GAMMA-RAY OBSERVATIONS OF CYGNUS X-1 ABOVE 1 MeV

We summarize in this Appendix all relevant observations and possible detections of Cyg X-1 above 1 MeV. We briefly describe the (so far) unique high-significance COMPTEL detection of Cyg X-1 up to 5–10 MeV in 1996 June. A short (less than 2 hr) episode of emission at TeV energies was detected by MAGIC in 2007. Finally, we discuss the gamma-ray event above 100 MeV detected by *AGILE* in pointing mode in 2009 October (Sabatini et al. 2010b), and focus on a new possible event detected by *AGILE* in spinning mode in early 2010 July coinciding with a dramatic spectral change from hard-to-soft states.

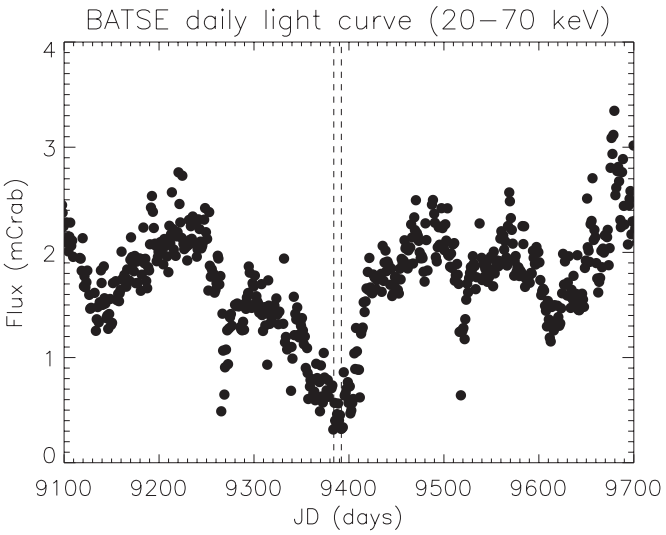

Figure 5. Soft spectral state of Cyg X-1 in 1994 January: BATSE light curve and COMPTEL observing period in dashed lines (VP 318.1, 1994 January). No emission was detected by COMPTEL or EGRET from Cyg X-1 above 1–10 MeV during this period.

A.1. Gamma-Ray Observations of Cygnus X-1 in the Soft State in 1994 and 1996: COMPTEL Data

Observations of Cyg X-1 during the soft state in the gamma-rays are scarce in the literature due to its intrinsic behavior: the source spent 90% of its time in the hard state during the last ∼20 years. During the operational period of *CGRO* (1991–2000) the instruments on board (BATSE, OSSE, COMPTEL, EGRET) observed the Cygnus region several times. Cyg X-1 was in a clear soft state in only two occasions: in 1994 January and in 1996 May. In both cases, *CGRO* pointed at the source with a target of opportunity (ToO) following the announcement of the hard-to-soft state transition. For the 1994 event (VP 318.1) all four *CGRO* instruments collected data, while for the 1996 one (VP 522.5) EGRET was switched off. Figure 5 shows the BATSE long-term light curve for the 1994 soft state and the *CGRO* ToO time period (marked by vertical dashed lines). No simultaneous soft X-ray monitoring was available at that time. COMPTEL did not detect any emission from Cyg X-1 for this period, and the upper limit was consistent with the $E^{-2.7}$ power law measured by both BATSE (Ling et al. 1997) and OSSE (Phlips et al. 1996).

Another interesting soft state episode occurred in 1996 June–July. Figure 6 shows the BATSE and simultaneous ASM long-term data around the 1996 Cyg X-1 soft state; the CGRO ToO viewing period is marked with vertical dashed lines. This observation, with a more favorable angle in the field of view, resulted in the first gamma-ray detection above ∼1 MeV of Cyg X-1. The hard X-ray spectral index was similar to that of the 1994 event (∼ −2.5). The overall intensity was also measured by OSSE to be higher than before by about a factor two (McConnell et al. 2002). This particular episode has been considered the "canonical" soft spectral state for a long time. The expectation from the model is that part of the emission

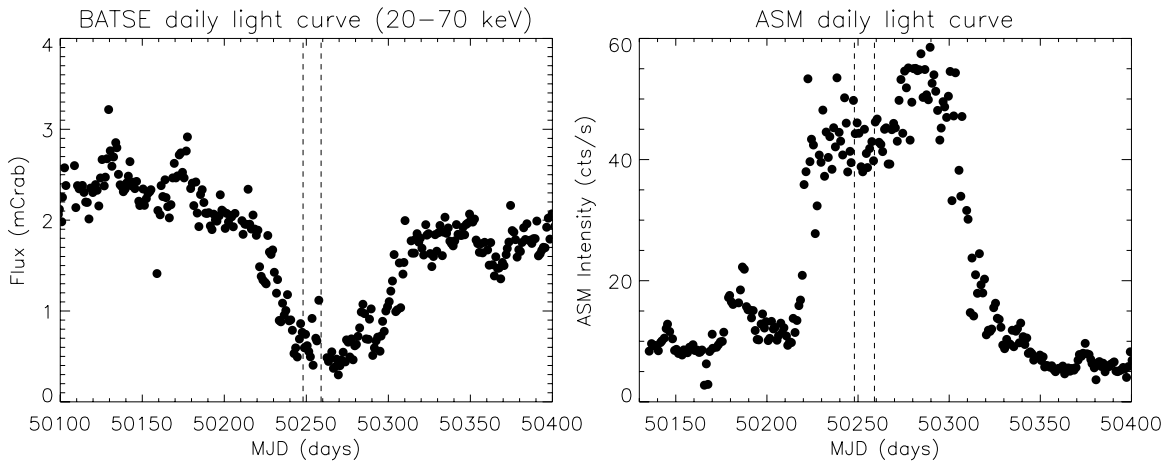

Figure 6. Soft spectral state of 1996 June: BATSE (left panel) and ASM *A*-band (right panel) light curves and COMPTEL observing period in dashed lines (VP 522.5). COMPTEL has detected Cyg X-1 in the range 1–10 MeV for this period (McConnell et al. 2002).

should also appear at energies $\geqslant$100 MeV, while *AGILE* shows that no emission is detected in this energy range, with an upper limit of 0.01 keV cm^{-2} s^{-1} (see Figure 4).

A.2. Transient Gamma-ray Episode of Cyg X-1 in the Hard State: MAGIC Observations

The Cyg X-1 hard state is described by a power law of typical spectral index 1.7 in the hard X-ray range, and a sharp energy cutoff around 150 keV. Therefore, significant gamma-ray emission is not expected in this spectral state. Until recently the higher energy data available in the literature were those of COMPTEL (McConnell et al. 2000, 2002), in agreement with this picture. EGRET provided only an upper limit for the source in the hard state (Hartman et al. 1999).

MAGIC reported for the first time an episode of transient TeV emission from Cyg X-1 in 2007 (Albert et al. 2007). The spectral state during this observation was a typical hard state spectrum and no unusual feature in the X-ray light curve and spectrum was noted. Quasi-simultaneous observations were carried out by *INTEGRAL*: the TeV detection coincides with the peak of a small X-ray flare just after a very fast rise in hard X-ray flux, but no obvious correlation between the X-ray and TeV emission was found (Malzac et al. 2008).

A.3. Transient Gamma-Ray Episode of Cygnus X-1 in the Hard State: AGILE Observations

As reported in Sabatini et al. (2010b), *AGILE* also detected above 100 MeV a fast ($\sim$1 day) transient event from Cyg X-1 in 2009 October during a hard state period. Although not simultaneous with the MAGIC event, the *AGILE* detection of a gamma-ray flare during a hard state, of the duration of the day or shorter, further suggests that additional non-thermal components may also appear in states previously believed to be characterized by a cutoff above a few MeV. The *AGILE* map of the 2009 October gamma-ray event is shown in Figure 7. Here we also show the multi-wavelength (AMI-LA, *MAXI*, and *Swift*-BAT) daily monitoring of Cyg X-1 during the gamma-ray flare detected by *AGILE*: as for the MAGIC flare, there is no evidence of detectable spectral changes or unusual features on the *day timescale*. It is however interesting to point out that a blind search analysis carried out in about 4 years of *Fermi* data shows that some low-significance activity is present in the gamma-ray data above 100 MeV during the periods of this gamma-ray flare (and the one discussed in Section A.4.1) reported by the *AGILE* Team for Cyg X-1. The analysis was supported by a statistical treatment of spurious detections and other periods of gamma-ray activity outside this ones and the one in Section A.4.1 reported by *AGILE* are probably spurious (A. Bodaghee 2012, private communication; see also Bodaghee 2012).

A.4. The Hard-to-soft State Transition of 2010 June–July: RXTE PCA Data and AGILE Observations

After having spent a long period from 2006 to mid 2010 in an extraordinary hard state (Nowak et al. 2012), on 2010 June 28 Cyg X-1 entered into a transitional state, passing from the hard to the soft state. A gradual spectral softening of the black hole during the period 2010 June 10–July 1 was announced by *MAXI*/GSC (Negoro et al. 2010) and the subsequent soft X-ray increasing emission was also reported by *RXTE*/ASM (Rushton et al. 2010a), confirming the transition of the source from the hard to the soft spectral state. The rapid fall in hard X-rays around 2010 June 29–July 1 was also reported by *Fermi*-GBM (Wilson-Hodge & Case 2010). A multi-wavelength campaign was triggered by the transition episode, providing a wealth of data from gamma-rays to radio (*MAXI*, Negoro et al. 2010; *RXTE*/ASM, Rushton et al. 2010a; *AGILE*, Sabatini et al. 2010a; *Fermi*-GBM, Wilson-Hodge & Case 2010; *SWIFT*, Evangelista et al. 2010; MERLIN, Rushton et al. 2010b; WRST, Tudose et al. 2010). All observations showed the source to be in an intermediate-soft state (Belloni et al. 1996). The source was detected to be in the soft state on the 2010 July 11 (Rushton et al. 2010b), and remained in this state until the end of 2011 April (Grinberg et al. 2011). Figure 8 shows a multi-wavelength long-term monitoring of the 2010–2011 soft state in the hard X-rays (BAT 15–50 keV), soft X-rays (*MAXI* 2–4 keV), and radio (AMI-LA 15 GHz). The vertical dot-dashed lines show the duration of a candidate episode of enhanced gamma-ray emission detected by *AGILE* during the remarkable hard-to-soft transition of 2010 July.

As reported in the main text, 19 pointed observations were performed by *RXTE*-PCA during the period 2010 June 19–July 31, for a net exposure time of about 68.5 ks, catching the source across the whole transition from the hard to the soft state. The observations were carried out in the binned data mode (B-2ms-8B-0-35-Q), with 1.95 ms bin size in the energy band 2.1–14.8 keV. In Figure 9 we plotted the X-ray power

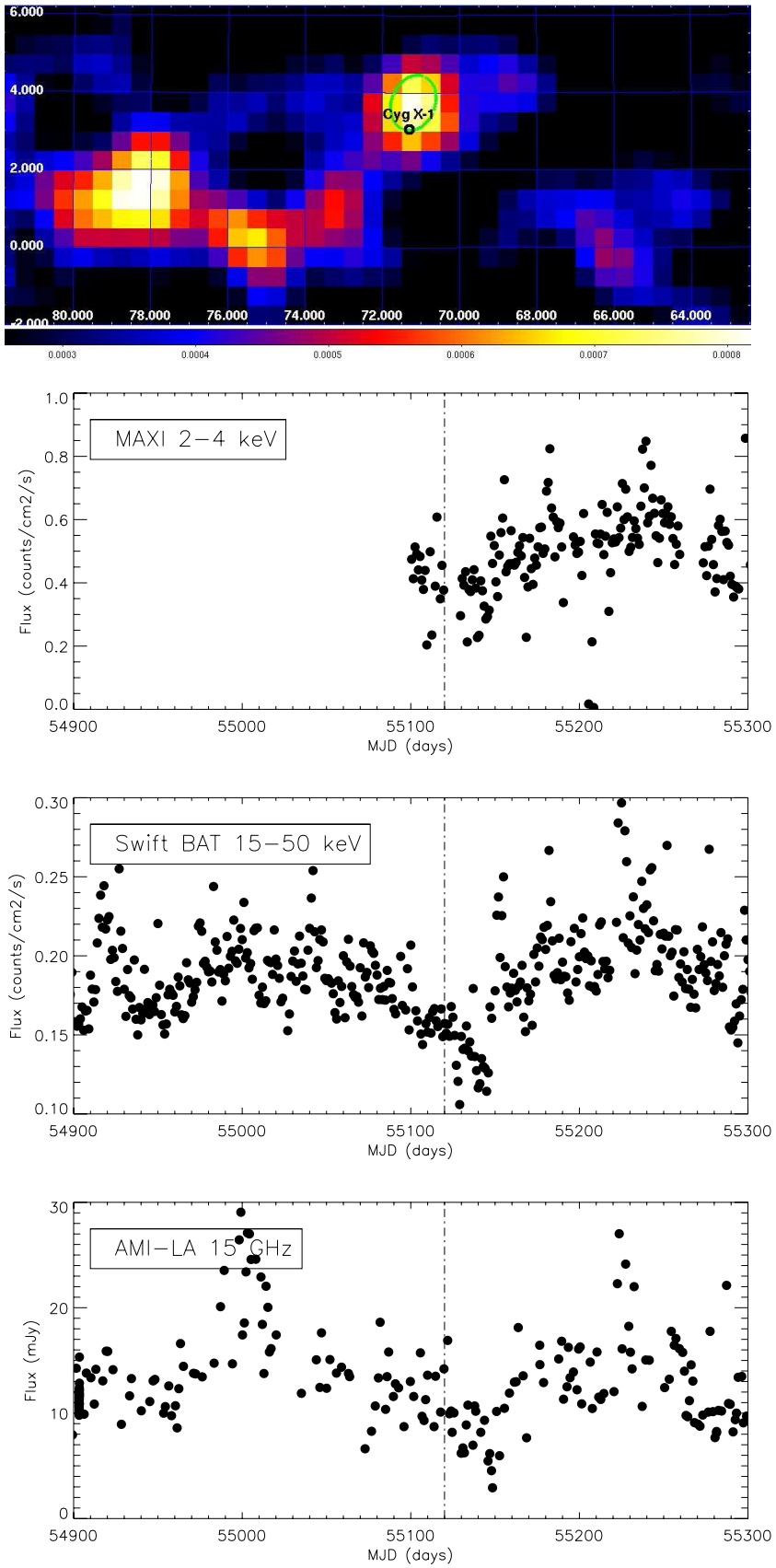

Figure 7. Hard spectral state. Upper panel: *AGILE* gamma-ray intensity map above 100 MeV of the Cygnus region in Galactic coordinates displayed with a three-bin Gaussian smoothing and a pixel size of 0.°5. The map is obtained by integrating data in the period 2009 October 15 UTC 23:13:36 to 2009 October 16 UTC 23:02:24. The black circle is the optical position of Cyg X-1 and the green contour is the *AGILE* 2σ confidence level. Other panels show multi-wavelength daily monitoring of Cyg X-1: *Swift*-BAT data in the 5–50 keV in the upper panel, *MAXI* data in the 2–4 keV in the middle panel, and AMI-LA data at 15 GHz in the lower panel. The vertical dashed lines show the duration of the gamma-ray event reported in Sabatini et al. (2010b).

(A color version of this figure is available in the online journal.)

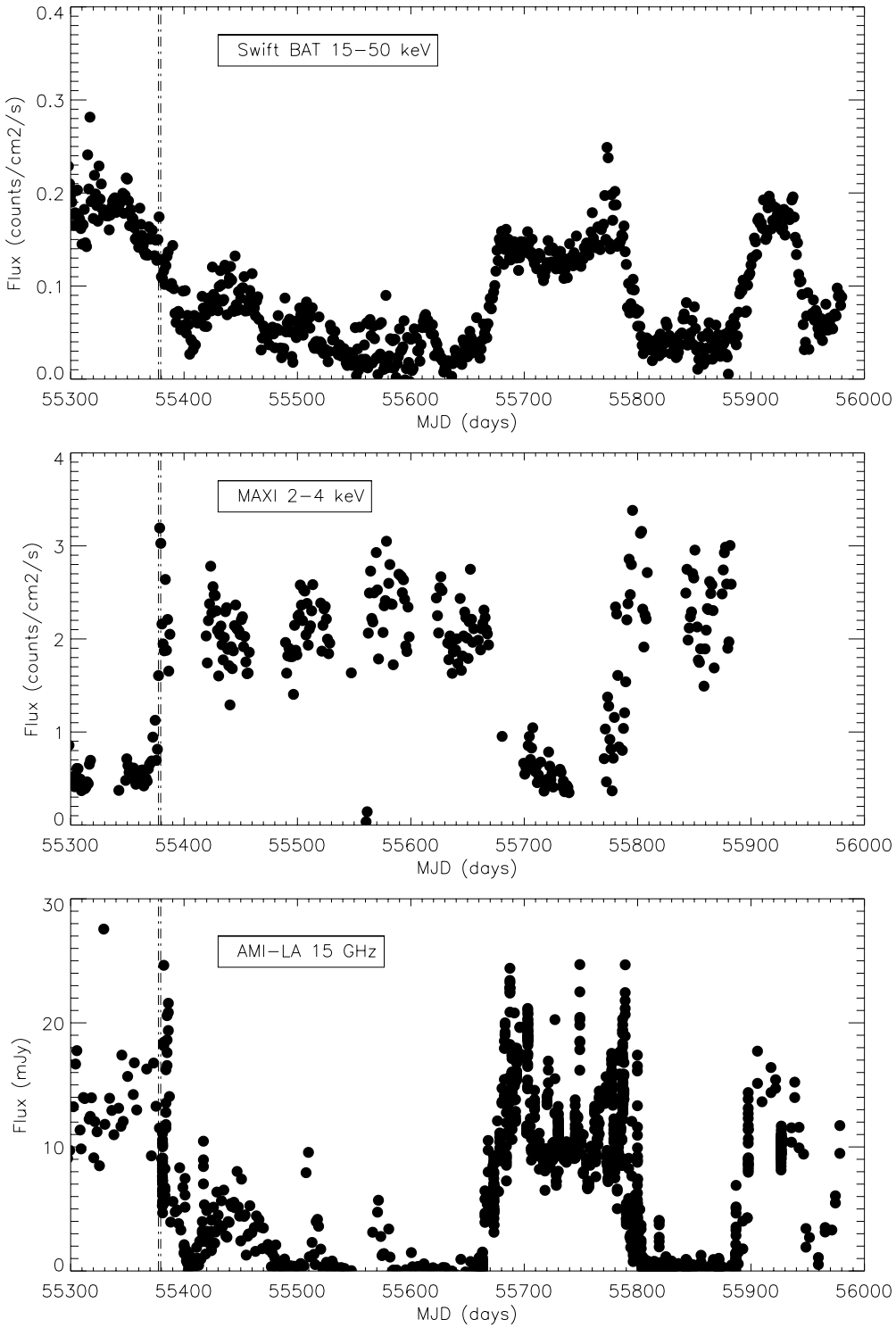

Figure 8. Multi-wavelength daily monitoring of Cyg X-1. Upper panel shows *Swift*-BAT data in the 15–50 keV energy range, middle panel *MAXI* data in the 2–4 keV band, and lower panel AMI-LA data at 15 GHz. Dashed lines refer to *AGILE* candidate flaring event.

spectrum (normalized to units of fractional squared rms) of the *RXTE*-PCA observation 95121-01-13-00 (2461 s net exposure) carried out on 2010 June 19 with $T_{\rm start}$ = 21:44:26.3 UT (black line), for observation 95121-01-14-00 (1730 s net exposure) performed on 2010 July 4 with $T_{\rm start}$ = 03:27:02.6 UT (red line) and for observation 95121-01-13-00 of 2010 July 22 with $T_{\rm start}$ = 07:40:40.28 UT. The *RXTE*-PCA data clearly show a variation in the noise components of the power spectra (PDS), with a decrease in the rms variability during the state change. The fractional rms was ∼8% on 2010 June 19, with a power spectrum showing band-limited noise between 0.3 Hz and 10 Hz (Figure 9, gray line), consistent with an intermediate state (see, e.g., Shaposhnikov & Titarchuk 2006). The fractional rms then dropped to about 4% on 2010 July 4, with a narrower noise component in the PDS which peaks at ∼3 Hz (Figure 9, left panel, green line), thus showing that the source had finally reached the soft state. We also plot in cyan the PDS of the July 22, clearly showing a super-soft state, as an example of the

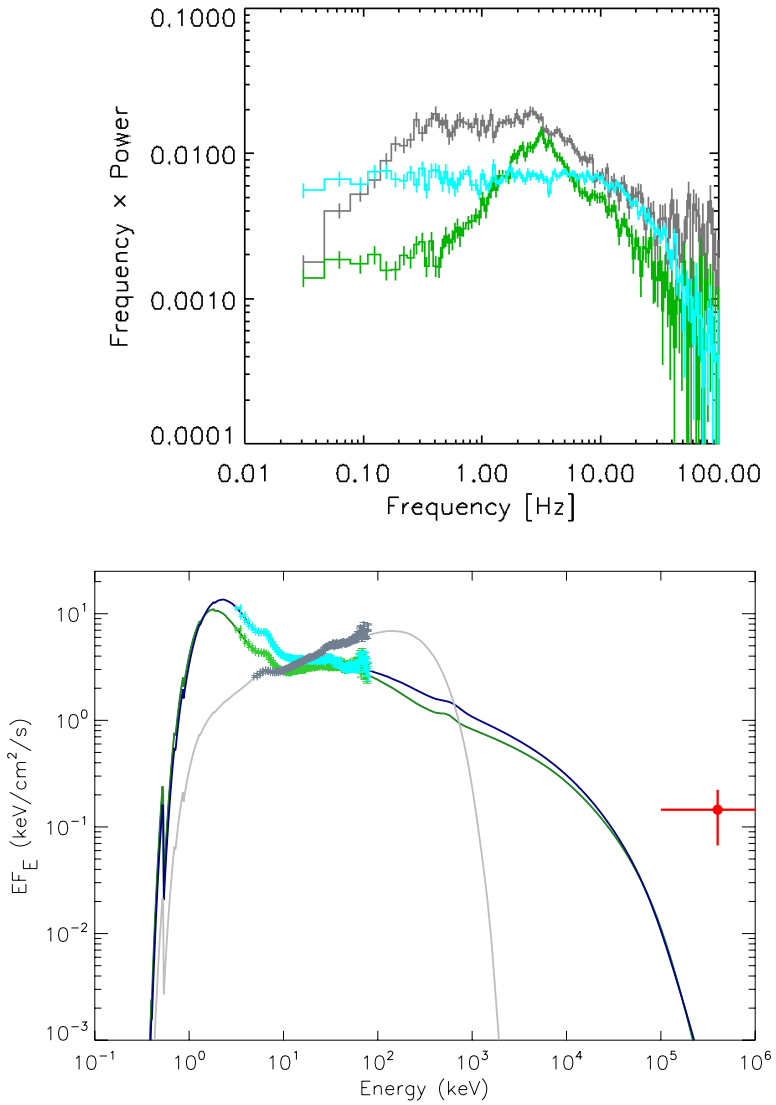

Figure 9. Top panel: power density spectra of Cyg X-1 before and after the spectral transition occurred at the end of 2010 June. *RXTE* PCA ToO data on 2010 June 19 is the gray curve; 2010 July 4 is the green curve; and 2010 July 22 is the cyan curve. Bottom panel: corresponding spectral energy distribution with *RXTE* PCA/HEXTE data for three days as in the top panel and *AGILE* flare in red.

(A color version of this figure is available in the online journal.)

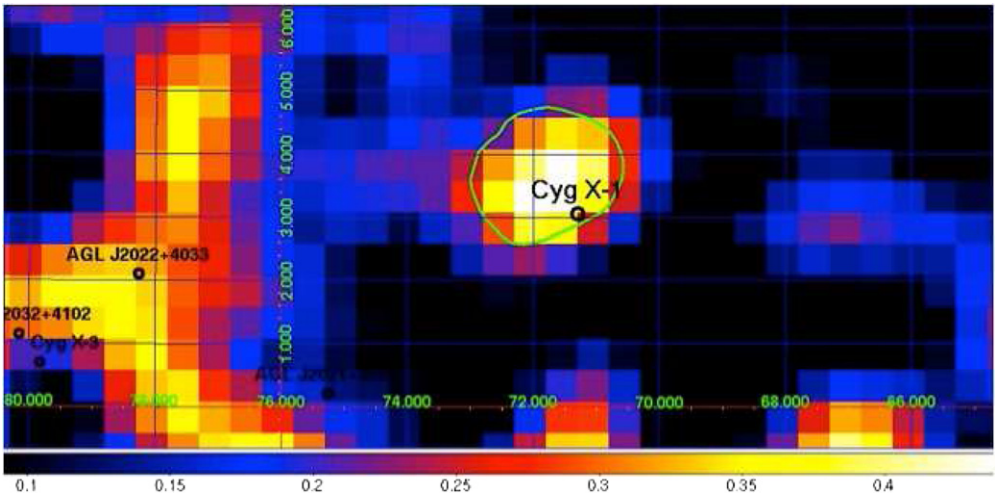

Figure 10. *AGILE* candidate transient event on 2010 June 30–July 2. Gamma-ray intensity map above 100 MeV of the Cygnus region in Galactic coordinates displayed with a three-bin Gaussian smoothing and a pixel size of $0.^{\circ}5$. The map is obtained by integrating data in the period: 2010 June 30 10:00 UT to 2010 July 2 10:00 UT. The nominal position of Cyg X-1 is overlaid in back and the error box of the detection is in green. The color bar scale is in units of photons cm^{-2} s^{-1}.

(A color version of this figure is available in the online journal.)

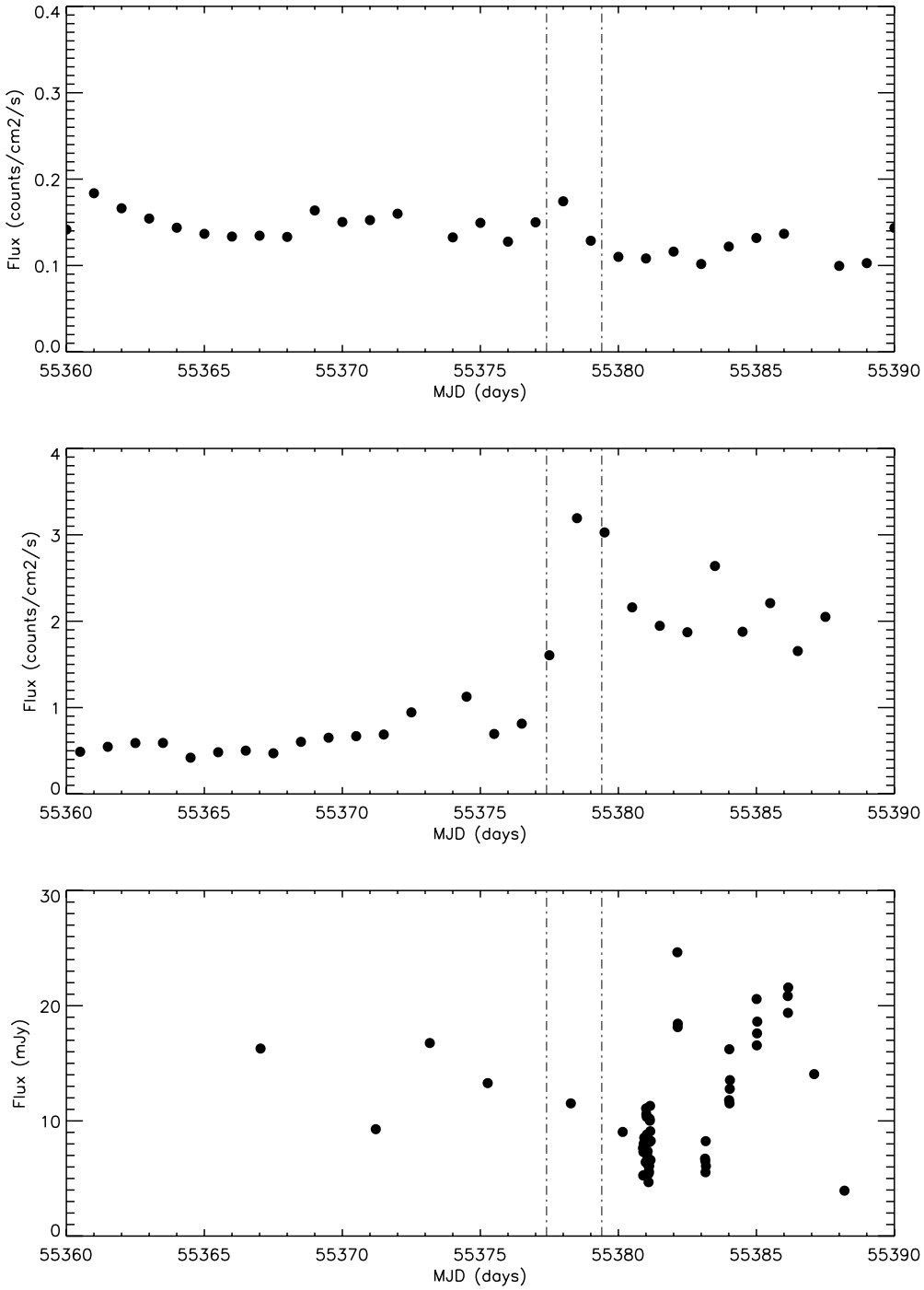

Figure 11. Multi-wavelength daily monitoring of Cyg X-1 focusing on the hard-to-soft transition of 2010 June. Upper panel shows *Swift*-BAT data in the 15–50 energy range, middle panel *MAXI* data in the 2–4 keV band, and lower panel AMI-LA data at 15 GHz. Dashed vertical lines refer to the *AGILE* candidate flaring event on 2010 June 30–July 2.

intrinsic variability present in the soft state period monitored by *AGILE*. Although not simultaneous with the *AGILE* candidate flaring event (see the next section), these observations are of particular interest to the gamma-ray data because they are a few days before and just after the possible gamma-ray detection, suggesting the coupling of transitional states with gamma-ray emission.

A.4.1. An AGILE Possible Detection of Cygnus X-1 at the Hard-to-soft Transition in 2010 July

We carried out an automatic search for transient gamma-ray emission in *AGILE* data during the whole 2010–2011 period, and found evidence of gamma-ray activity during the 2010 hard-to-soft spectral transition. Based on previous claims of gamma-ray detections of Cyg X-1 on short timescales by MAGIC (Albert et al. 2007) and *AGILE* (Sabatini et al. 2010b), we searched for events occurring on short timescales (2 days). A relatively weak, i.e., low statistical significance, but interesting gamma-ray enhancement occurs exactly at the hard-to-soft transition at the end of 2010 June. Integrating from 2010 June 30 10:00 UT to 2010 July 2 10:00 UT, the maximum likelihood analysis yields a flux excess above 100 MeV of $F_\gamma = 145 \pm 78 \times 10^{-8}$ photons cm^{-2} s^{-1} with a 3σ statistical significance. Figure 10 shows the *AGILE*

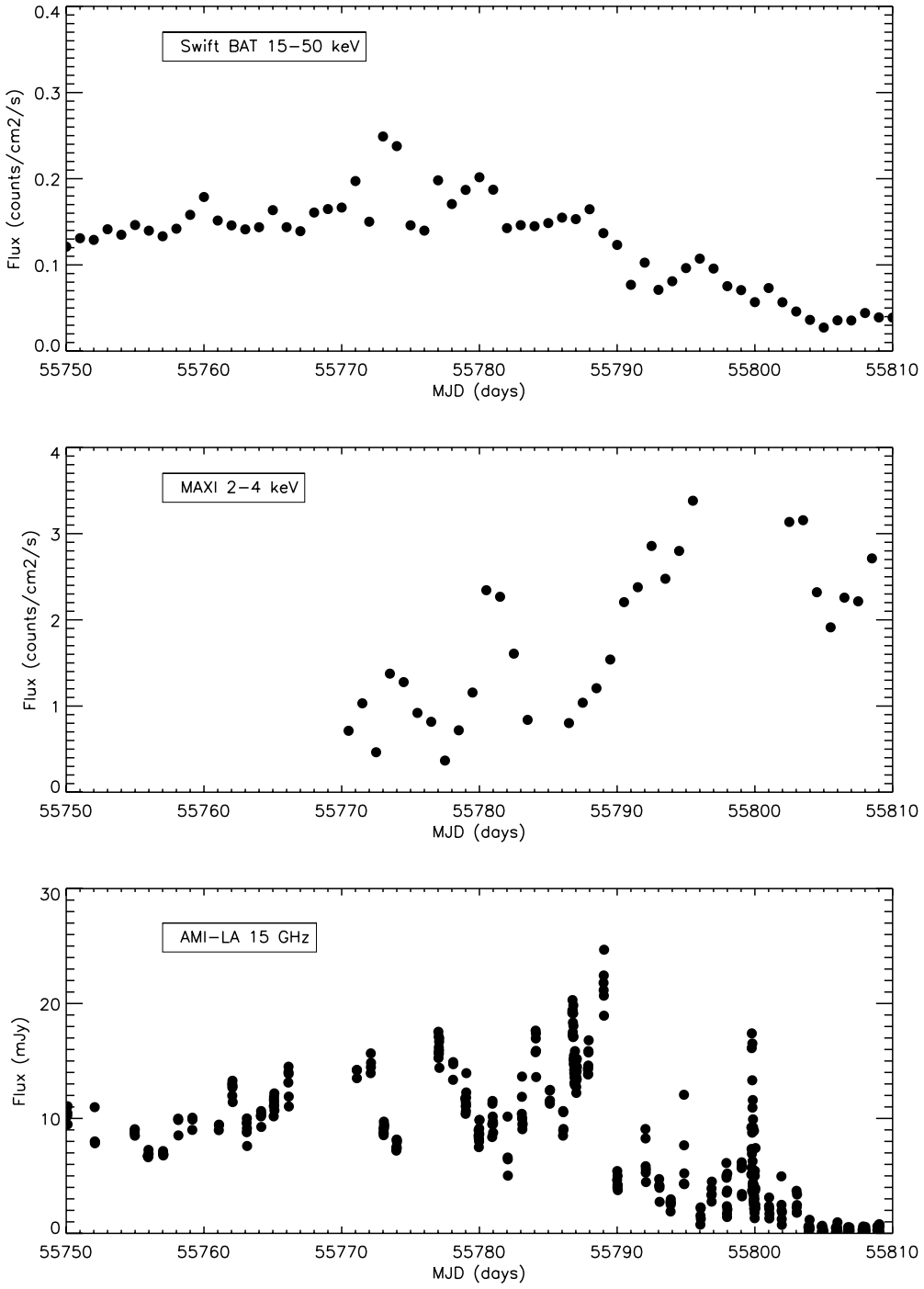

Figure 12. Multi-wavelength daily monitoring of Cyg X-1 focusing on the hard-to-soft transition of 2011 January. Upper panel shows *Swift*-BAT data in the 15–50 keV energy range, middle panel *MAXI* data in the 2–4 keV band, and lower panel AMI-LA data at 15 GHz.

gamma-ray intensity map of the Cygnus region above 100 MeV for this period. Although not simultaneous, we think it is interesting to show in Figure 9 the *AGILE* data point for the candidate flare with the extreme models (model-1 and model-2) discussed in the main text. For comparison, we also show in gray the *RXTE* PCA/HEXTE data for the ToO observation of 2010 June 19, i.e., 10 days before the *AGILE* candidate flare, when Cyg X-1 was in a hard/intermediate state (we plot a representative model with $l_{\rm nth}/l_h = 0$ for this case).

Although the statistical significance of the gamma-ray enhancement detected by *AGILE* is low (because of the poor statistics obtainable for short events by *AGILE* in spinning mode), it is interesting to discuss this candidate event in a multi-wavelength perspective. Figure 8 shows a long-term monitoring in hard X-rays (*Swift*-BAT, upper panel), soft X-rays (*MAXI* in the 2–4 keV band, middle panel), and radio (AMI-LA 15 GHz band, lower panel); the dashed lines show the *AGILE* detection. Interestingly, the gamma-ray flare happens to be simultaneous with the definitive transition to the soft state, and anticipates by about 2 days an "anomalous" intense radio flare detected well in the soft state (Rushton et al. 2012), occurring therefore when shocks are possibly predicted to be formed within the jet

(Fender et al. 2004). As already mentioned in Appendix A.3, a blind search analysis supported by a statistical treatment of spurious detections shows that some low-significance activity is also present in the *Fermi* gamma-ray data during the period of this gamma-ray flare (A. Bodaghee 2012, private communication; see also Bodaghee 2012).

Figure 11 shows the detailed transition as detected in the hard X-rays (BAT), 2–4 keV X-rays (*MAXI*), and radio (AMI-LA). The time period of enhanced gamma-ray emission above 100 MeV possibly detected by *AGILE* is marked by vertical dashed lines.

We also searched for gamma-ray activity from Cyg X-1 coinciding with other interesting spectral transitions as shown in Figure 8. However, there is no evidence of enhanced emission in the data ($F_{\rm UL} \sim 200 \times 10^{-8}$ photons cm^{-2} s^{-1} for 2 days integration). Figure 12 shows the detail of the other recent hard-to-soft transition which occurred in 2011 January and led to another prolonged soft state (∼MJD: 55800–55890). We note that in this case the hard-to-soft transition occurs on a timescale of several days, i.e., much longer than the sharp transition recorded in 2010 July coinciding with the *AGILE* candidate event.

REFERENCES

Abdo, A. A., Ackermann, M., Ajello, M., et al. 2009, Sci, 326, 1512
Albert, J., Aliu, E., Anderhub, H., et al. 2007, ApJL, 665, L51
Barbiellini, G., Fedel, G., Liello, F., et al. 2002, NIMPA, 490, 146
Belloni, T., Mendez, M., van der Klis, M., et al. 1996, ApJL, 472, L107
Bodaghee, A. 2012, http://fermi.gsfc.nasa.gov/science/mtgs/symposia/2012/program/parallel_b2.html
Brocksopp, C., Fender, R. P., Larionov, V., et al. 1999, MNRAS, 309, 1063
Bulgarelli, A., Argan, A., Barbiellini, G., et al. 2010, NIMPA, 614, 213
Bulgarelli, A., Chen, A. W., Tavani, M., et al. 2012a, A&A, 540, 79
Bulgarelli, A., Tavani, M., Chen, A. W., et al. 2012b, A&A, 538, 63
Caballero-Nieves, S. M., Gies, D. R., Bolton, C. T., et al. 2009, ApJ, 701, 1895
Chen, A., Piano, G., Tavani, M., et al. 2011, A&A, 525, 33
Collmar, W. 2003, in X-Ray and Gamma-Ray Astrophysics of Galactic Source, 4th AGILE Science Workshop, ed. M. Tavani, A. Pellizzoni, & S. Vercellone (Rome: ARACNE Editrice S.r.l), 177
Coppi, P. S. 1999, in ASP Conf. Ser. 161, High Energy Processes in Accreting Black Holes, ed. J. Poutanen & RolandSvensson (San Francisco, CA: ASP), 375
Coppi, P. S. 2004, in AIP Conf. Proc. 714, X-Ray Timing 2003: Rossi and Beyond, ed. P. Kaaret, F. K. Lamb, & J. H. Swank (Melville, NY: AIP), 79
Corbel, S., Dubus, G., Tomsick, J. A., et al. 2012, MNRAS, 421, 2947
Del Monte, E., Feroci, M., Evangelista, Y., et al. 2010, A&A, 520, 67
Del Santo, M., Malzac, J., Belmont, R., Bouchet, L., & De Cesare, G. 2013, MNRAS, 430, 209
Evangelista, Y., Campana, R., Del Monte, E., et al. 2010, ATel, 2724, 1
Fender, R. P. 2001, MNRAS, 322, 31
Fender, R. P., Belloni, T. M., & Gallo, E. 2004, MNRAS, 355, 1105
Fender, R. P., Pooley, G. G., Durouchoux, P., Tilanus, R. P. J., & Brocksopp, C. 2000, MNRAS, 312, 853
Fender, R. P., Stirling, A. M., Spencer, R. E., et al. 2006, MNRAS, 369, 603
Feroci, M., Costa, E., Soffitta, P., et al. 2007, NIMPA, 581, 728
Frontera, F., Palazzi, E., Zdziarski, A. A., et al. 2001, ApJ, 546, 1027
Gallo, E., Fender, R. P., Kaiser, C., et al. 2005, Natur, 436, 819
Gallo, E., Fender, R. P., & Pooley, G. G. 2003, MNRAS, 344, 60
Gierlinski, M., & Zdziarski, A. A. 2003, MNRAS, 343, 84
Gierlinski, M., Zdziarski, A. A., Done, C., et al. 1997, MNRAS, 288, 958
Gierlinski, M., Zdziarski, A. A., Poutanen, J., Coppi, P. S., Ebisawa, K., & Johnson, W. N. 1999, MNRAS, 309, 496
Gleissner, T., Wilms, J., Pooley, G. G., et al. 2004, A&A, 425, 1061
Golenetskii, S., Aptekar, R., Frederiks, D., et al. 2003, ApJ, 596, 1113
Grinberg, V., Boeck, M., Pottschmidt, K., et al. 2011, ATel, 3307, 1
Hartman, R. C., Bertsch, D. L., Bloom, S. D., et al. 1999, ApJS, 123, 79
Herrero, A., Kudritzki, R. P., Gabler, R., et al. 1995, A&A, 297, 556
Jourdain, E., Roques, J. P., & Malzac, J. 2012, ApJ, 744, 64
Labanti, C., Marisaldi, M., Fuschino, F., et al. 2006, Proc. SPIE, 6266, 110
Laurent, P., Rodriguez, J., Wilms, J., et al. 2011, Sci, 332, 438
Ling, J. C., Wheaton, W. A., Wallyn, P., et al. 1997, ApJ, 484, 375
Malzac, J., Belmont, R., & Fabian, A. C. 2009, MNRAS, 400, 1512
Malzac, J., Lubinski, P., Zdziarski, A. A., et al. 2008, A&A, 492, 527
Malzac, J., & Renaud, B. 2010, IJMPD, 19, 369
Mattox, J. R., Bertsch, D. L., Chiang, J., et al. 1996, ApJ, 461, 396
McConnell, M. L., Bennett, K., Bloemen, H., et al. 1997, in AIP Conf. Proc. 410, The Fourth Compton Symposium (Melville, NY: AIP), 829
McConnell, M. L., Ryan, J. M., Collmar, W., et al. 2000, in Bulletin of the American Astronomical Society 29, 190th AAS Meeting (Washington, DC: AAS)
McConnell, M. L., Zdziarski, A. A., Bennett, K., et al. 2002, ApJ, 572, 984
Mirabel, I. F., Claret, A., Cesarsky, C. J., Boulade, O., & Cesarsky, D. A. 1996, A&A, 315, L113
Negoro, H., Kawai, N., Kawasaki, Y. U. K., et al. 2010, ATel, 2711, 1
Nowak, M. A., Wilms, J., Pottschmidt, K., & Markoff, S. 2012, MmSAI, 83, 202
Orosz, J. A., McClintock, J. E., Aufdenberg, J. P., et al. 2011, ApJ, 742, 84
Pandey, M., Rao, A. P., Pooley, G. G., et al. 2006, A&A, 447, 525
Perotti, F., Fiorini, M., Incorvaia, S., Mattaini, E., & Sant'Ambrogio, E. 2006, NIMPA, 556, 228
Perucho, M., & Bosch-Ramon, V. 2008, A&A, 482, 917
Phlips, B., Jung, G. V., Leising, M. D., et al. 1996, ApJ, 465, 907
Piano, G., Tavani, M., Vittorini, V., et al. 2012, A&A, 545, 110
Pooley, G. G., Fender, R. P., & Brocksopp, C. 1999, MNRAS, 302, L1
Pottschmidt, K., Wilms, J., Nowak, M. A., et al. 2003, A&A, 407, 1039
Poutanen, J., & Coppi, P. S. 1998, PhST, 77, 57
Prest, M., Barbiellini, G., Bordignon, G., et al. 2003, NIMPA, 501, 280
Rahoui, F., Lee, J. C., Heinz, S., et al. 2011, ApJ, 763, 63
Romero, G. E., Torres, D. F., Kaufman Bernad, M. M., & Mirabel, I. F. 2003, A&A, 410, L1
Rushton, A., Dhawan, V., Fender, R., et al. 2010a, ATel, 2714, 1
Rushton, A., Evangelista, Y., Paragi, Z., et al. 2010b, ATel, 2734, 1
Rushton, A., Miller-Jones, J. C. A., Campana, R., et al. 2012, MNRAS, 419, 3194
Rushton, A., Miller-Jones, J., Paragi, Z., et al. 2011, PoS (arXiv:1101.3322v1)
Russell, D. M., Fender, R. P., Gallo, E., & Kaiser, C. 2007, MNRAS, 376, 1341
Sabatini, S., Striani, E., Verrecchia, F., et al. 2010a, ATel, 2715, 1
Sabatini, S., Tavani, M., Striani, E., et al. 2010b, ApJ, 712, 10
Shaposhnikov, N., & Titarchuk, L. 2006, ApJ, 643, 1098
Shaposhnikov, N., & Titarchuk, L. 2007, ApJ, 663, 445
Stirling, A. M., Spencer, R. E., de la Force, C. J., et al. 2001, MNRAS, 327, 1273
Tavani, M., Barbiellini, G., Argan, A., et al. 2008, A&A, 502, 995
Tavani, M., Bulgarelli, A., Piano, G., et al. 2009, Natur, 462, 620
Tudose, V., Pooley, G., Rushton, A., et al. 2010, ATel, 2755, 1
Wilson-Hodge, C., & Case, G. 2010, ATel, 2721, 1
Zdziarski, A. A. 2012, MNRAS, 422, 1750
Zdziarski, A. A., & Gierlinski, M. 2004, PThPS, 155, 99
Zdziarski, A. A., Lubinski, P., & Sikora, M. 2012, MNRAS, 423, 663
Zdziarski, A. A., Poutanen, J., Paciesas, W. S., & Wen, L. 2002, ApJ, 578, 357
Zdziarski, A. A., Skinner, G. K., Pooley, G. G., & Lubinski, P. 2011, MNRAS, 416, 1324
Zhang, S. N., Cui, W., Harmon, B. A., et al. 1997a, ApJL, 477, L95
Zhang, S. N., Mirabel, I. F., Harmon, B. A., et al. 1997b, in AIP Conf. Proc. 410, The Fourth Compton Symposium (Melville, NY: AIP), 141